International Journal of Multidisciplinary Advanced Research Trends (IJMART)
A Peer Reviewed (Referred) International Journal
http://ijmart.in/
Email: editor.ijmart@gmail.com
ISSN : 2349-7408
Vol. VII, Issue 2(1)
(AUGUST - 2020)

RESEARCH ARTICLE

VISIBLE LIGHT PHOTOCATALYTIC DEGRADATION OF CONGO RED AND ALIZARIN RED DYES WITH SILVER CAPPED COPPER TUNGSTATE NANO COMPOSITE

SURESH DODDA
SUPRIYA GADI
SWAPNA DUPPATI
RAMAKRISHNA REDDY CHINNAM
PAUL DOUGLAS SANASI
Department of Engineering Chemistry, AU College of Engineering (A),
Andhra University, Visakhapatnam - 530 003. AP

SURESH DODDA

ABSTRACT

Ag-$CuWO_4$ nano composite has been investigated for photocatalytic degradation with Congo Red and Alizarine Red dyes under visible light irradiation. The XRD, FESEM, EDS studies illustrates the morphology and structure of the prepared sample in detail. The complete degradation of Congo red dye took place in 60 minutes and Alizarine red dye in 80 minutes under visible light irradiation with Ag-$CuWO_4$ as the photo catalyst. This result suggests that as-obtained nano crystalline Ag-$CuWO_4$ composite is found as favourable material having high potential to be used for photo catalytic applications under visible light

Introduction

In recent years a lot of study is made to develop semiconductor based photocatalysts with enormous photocatalytic activity to save the environment, employing procedures like disinfecting water, purifying air, remediating waste water, etc. Its powerful oxidizing behavior, chemical inactivity, economic viability and non-poisonous nature makes it an effective technique [1-3].Several oxides and tungstates of metals are effective photocatalysts due to their unique electronic structure, charge transport characteristics and light absorption properties. Transition metal tungstates are inorganic materials having prominent application in different sectors. These are used in fluorescent lights and laser lamps, owing to their tremendous electrical conductance. They find use as humidity sensors and catalysts. $CuWO_4$ has significant technical uses in scintillate detectors, laser hosts, optical fibers and photon-odes. [4-5]. Many oxide materials are synthesized by solid-state metathetic approach. Oxides of $K_2La_2Ti_3O_{10}$, $Ca_2La_2CuTi_2O_{10}$ which belong to Ruddleson-

International Journal of Multidisciplinary Advanced Research Trends (IJMART)
A Peer Reviewed (Referred) International Journal
http://ijmart.in/
Email: editor.ijmart@gmail.com
ISSN : 2349-7408
Vol. VII, Issue 2(1) (AUGUST - 2020)

Popper type of substances, ABO_3 perovskite type of substances like $LaMO_3$ (M = Co, Mn), $ATiO_3$ (A = Ca, Sr and Ba) and double perovskites like $Ba_3MM'_2O_9$ *(M = Mg, Ni, Zn; M' = Nb, Ta)were synthesized by* this method, by Gopalakrishnan et. al. [6-9]. Using the same approach, oxide compounds of Zr, Hf and Cu *were synthesized by* Kaner et. al. [10, 11]. At high pressure, only wolframite-type monoclinic structure is exhibited by $CuWO_4$ crystals[12]. $CuWO_4$ is also used in water splitting and photocatalytic reactions [13, 14]. Around 650 varieties of disease causing microorganisms are killed by silver, which is a secure inorganic agent acting against bacteria [15]. Owing to their antimicrobial properties, there is growing interest in silver nanoparticles [16]. Various studies project them as future generation antimicrobial agents [17].

Silver nanoparticles exhibit distinguishing electrical, optical and biological properties and hence find applications in catalytic reactions, imaging, bio-sensing, delivery of drugs, fabricating nano devices and also has medicinal applications [18, 19].The designing of dependable procedures to synthesise nanoparticles is an important aspect of nanotechnology [20].Their synthesis by physical and chemical procedures might be laborious, expensive and pose considerable environmental concern [21, 22]. The high reactivity of the metal nanoparticles depends on two conditions. One is they cannot be protected from oxidation, as they do not have compact organic surface layer. The other condition is that the redox potential of silver shifts to negative values as the size of the particles decrease. Also silver clusters can store electrons upon charge injection from reducing species.

Copper tungstate nano particles show strong interactions with the silver nano particles and hence silver nano particles are adsorbed on them, forming silver capped copper tungstate nano composite. The photo catalytic capability of this Ag-$CuWO_4$ composite was studied by the degrading Congo red and Alizarin red dyes irradiated by visible-light, and the data is depicted in **Figure 10** and **Figure 11.**

$CuWO_4$ has a direct band gap which is placed near the optical value of the solar spectrum and the higher energy of CB (Conduction Band), which gives the photo electrons a strong reducing capability and silver nano particles exhibit remarkable electrical transport property. As a result, remarkable electrical transport property is also exhibited by the Ag-$CuWO_4$ composite. For the enhanced photo catalytic activity of Ag-$CuWO_4$ composite, a reaction mechanism can be given. A part of silver nano particles act as a carrier of photons and conducts electrons to the copper tungstate's surface. This enhances the separation of the electron-hole pairs and efficiency of photo catalysis. It serves as an electron acceptor and transporter.

In the present work, a facile metathetic synthesis of $CuWO_4$, nano $CuWO_4$ and Ag-$CuWO_4$ nano composite has been described. XRD, FE-SEM and EDAX were used to characterize the morphology and composition. The degradation of Congo Red and Alizarin Red dyes has been studied by performing photo catalysis using the prepared materials.

Characterisation of the Catalyst Ag-$CuWO_4$ nano composite

X-Ray Diffraction of Silver Nanoparticles

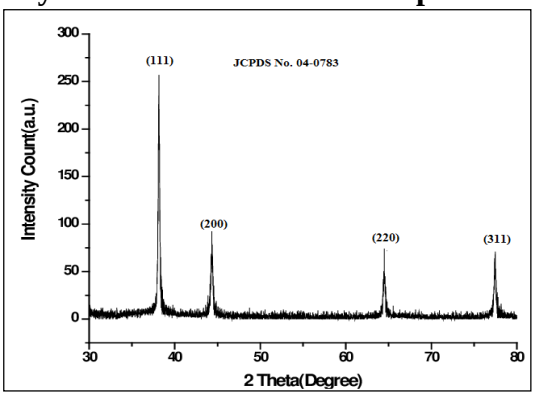

Figure 1: XRD-Spectrum of Silver nanoparticles

International Journal of Multidisciplinary Advanced Research Trends (IJMART)
A Peer Reviewed (Referred) International Journal
http://ijmart.in/
Email: editor.ijmart@gmail.com
ISSN : 2349-7408
Vol. VII, Issue 2(1)
(AUGUST - 2020)

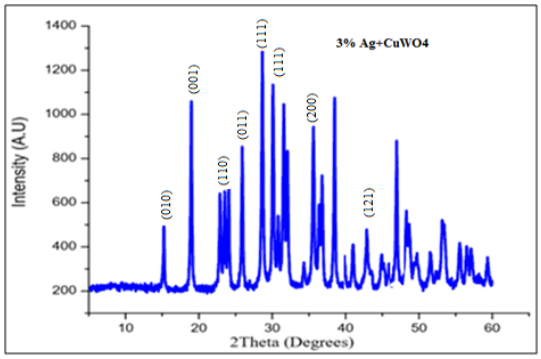

Figure 2: XRD-Spectrum of Ag-$CuWO_4$ nano composite

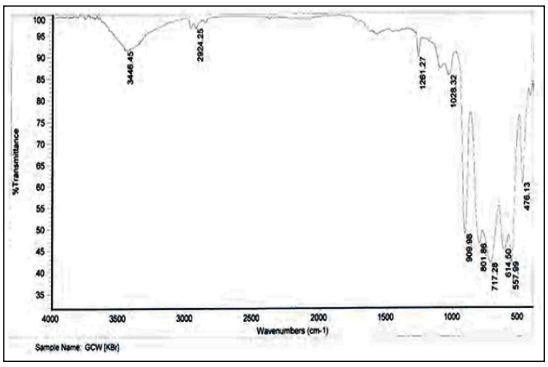

Figure 3: FT-IR spectrum of $CuWO_4$

Figure 1 shows the X-Ray Diffraction plot of silver nano particles and its peaks excellently match with the distinctive peaks. **Figure 2** shows the X-Ray Diffraction graph of Ag-$CuWO_4$ nano composite. The peaks of the composite excellently match with the distinctive peaks of $CuWO_4$. While a distinct peak for pure silver nano particles was noticed at 2θ =38.4 (111) and 45.3° (200) (**Figure 1**), this peak relevant to Ag is noticed in Ag-$CuWO_4$ plot [23]. Representative XRD analysis was used to confirm the phase purity of the as-synthesized substances. As shown in **Figure 2**, the as-prepared powder samples have similar tapered distinctive peaks placed at 15.1°, 19.2°, 23.8°, 24.9°, 29.2°, 31.6°, 36.7° and 43.8°, which agree well with the (010), (001), (110), (0 11), (111), (111), (200) and (121) planes, respectively. All these crystal planes are excellently match with the patterns typical of triclinic phase $CuWO_4$ (JCPDS No 80-1918)[24].

FT-IR Spectrum of the Catalyst

Figure 3 shows the FT-IR spectrum of $CuWO_4$. Owing to the OH- stretching vibrations of free and hydrogen-bonded hydroxyl groups, the spectrum exhibits a broad band near 3446 cm^{-1}.Along the direction, the Cu-O stretching vibration results in the band at 614 cm^{-1} and the peak at 476 cm^{-1} and the presence of W-OH bond causes the peak at 1028 cm^{-1} [25].

Composition and Morphology Study

The FE-SEM of silver-copper tungstate nano composite is shown in **Figure 4**. FE-SEM characterization is used to examine the nano structures and sample morphologies, which reveals that micro structured copper tungstate particles have a coarse surface, with various non-uniform particles berthed on the surface of copper tungstate. Thus it could be concluded that nano particles in sizes of <50 nm in diameter are present in the prepared sample. Also the presence of Copper, Tungsten, Oxygen and silver was demonstrated by the EDS spectrum. This substantiates the proper formation of 3% silver-copper tungstate nano composite. The composition of 59.49 % W, 20.55 % O, 20.41 % Cu and 2.89 % Ag (%wt.) was shown by EDS analysis.

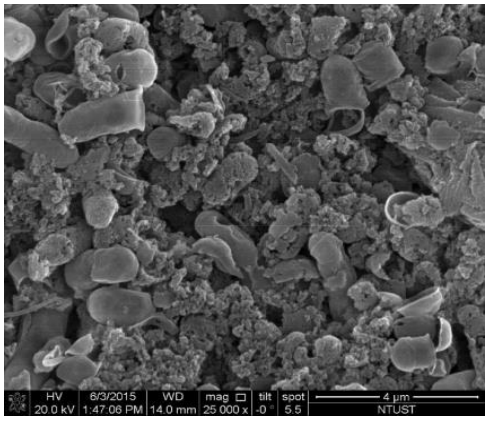

4-A

International Journal of Multidisciplinary Advanced Research Trends (IJMART)
A Peer Reviewed (Referred) International Journal
http://ijmart.in/
Email: editor.ijmart@gmail.com
ISSN : 2349-7408
Vol. VII, Issue 2(1)
(AUGUST - 2020)

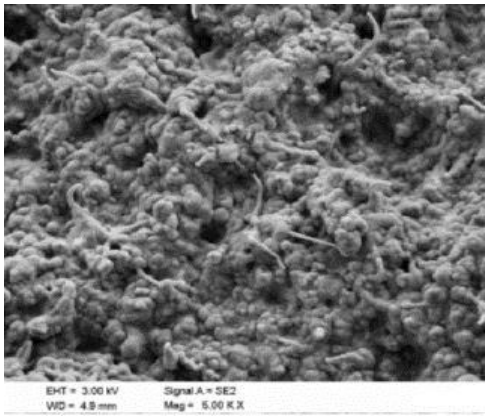

4-B

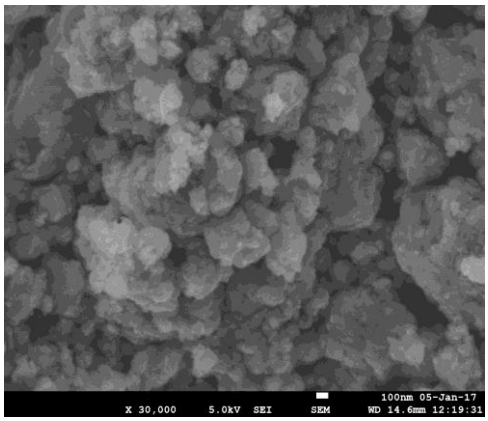

4-C

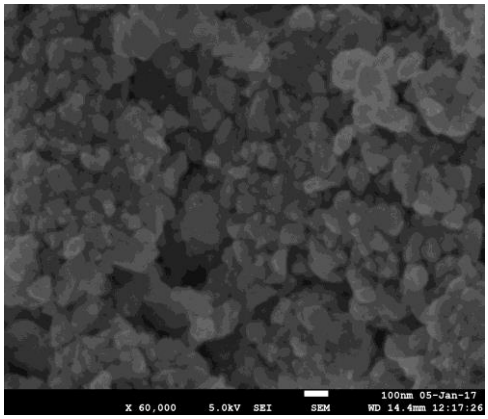

4-D

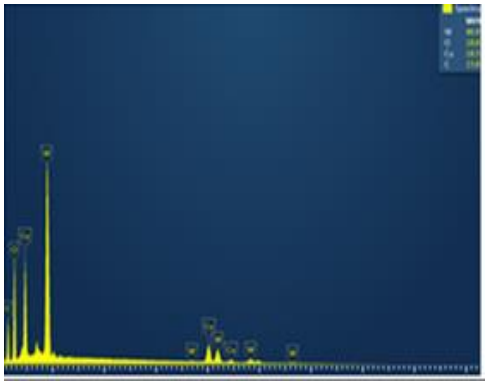

4-E

Element	Weight%
Ag	2.89
O	20.55
Cu	20.41
W	59.49
Total	100

Figure 4: FE-SEM micrographs of 3% Ag-$CuWO_4$ nano composite and EDS spectra

UV Diffuse Reflectance Spectral Studies

UV-Diffuse Reflectance Spectroscopy is used to evaluate the optical aspects of pure $CuWO_4$, nano $CuWO_4$ and Ag-$CuWO_4$ nano composite as shown in **Figure 5 – Figure 8.** The λ_{max} for micro sized copper tungstate was at 290 nm and the computed band gap was 4.5 eV (**Figure 5**).The λ_{max} for the nano copper tungstate was at 580 nm and the band gap has come down to 2.5 eV, which is shown in **Table 1**. and **Figure 6**. The absorption in the visible light region can take place from a band gap transition from macro to nano size, as indicated by the sharp decrease in the band gap of nano $CuWO_4$. Photon energy activates the electrons on the valence band and they jump to the conduction band [26].The silver nano particles were not engulfed into the lattice of copper tungstate and they simply were adsorbed on the surface. For the silver-copper tungstate nano

International Journal of Multidisciplinary Advanced Research Trends (IJMART)
A Peer Reviewed (Referred) International Journal
http://ijmart.in/
Email: editor.ijmart@gmail.com
ISSN : 2349-7408
Vol. VII, Issue 2(1)
(AUGUST - 2020)

composite, theλ_{max} is noticed at 580 nm and the band gap is noted to be 2.2 eV as shown in **Figure 7** and **Figure 8**.

Planck-Einstein Relation is given below, which relates the band gap of a given solid and the wavelength of light reflected by it. E is the band gap energy in joules, h is Planck's constant (6.63×10^{-34}J s) and $\nu$is frequency in Hz.

$$E_g = h\nu = \frac{hc}{\lambda} \qquad (Eq.3.1)$$

The wavelength of the substance is computed from the graph of wavelength(λ) versus absorbance, and band gap is known from the following formula, where λ is the wavelength of the substance from the graph. E_g is the bandwidth to be determined.

$$Eg = \frac{1240}{\lambda(nm)} \qquad (Eq.3.2)$$

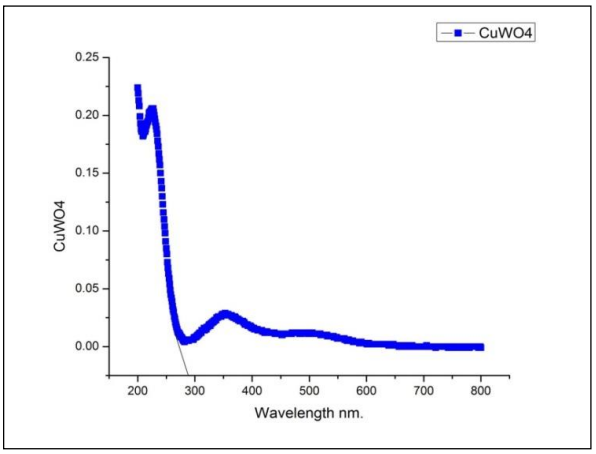

Figure 5: Band gap spectrum of $CuWO_4$ (prepared by metathesis)

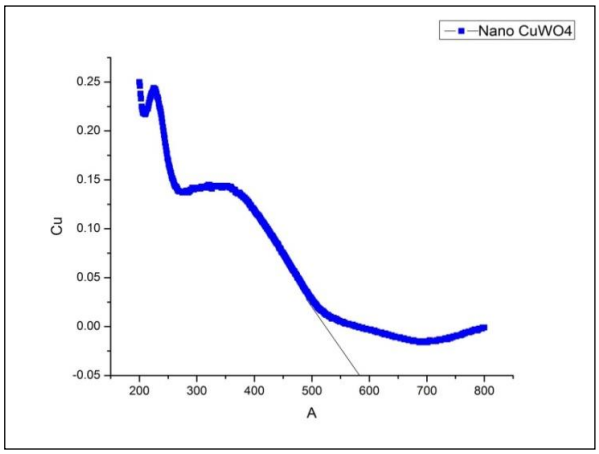

Figure 6: Band gap spectrum of $CuWO_4$ (after low energy ball milling)

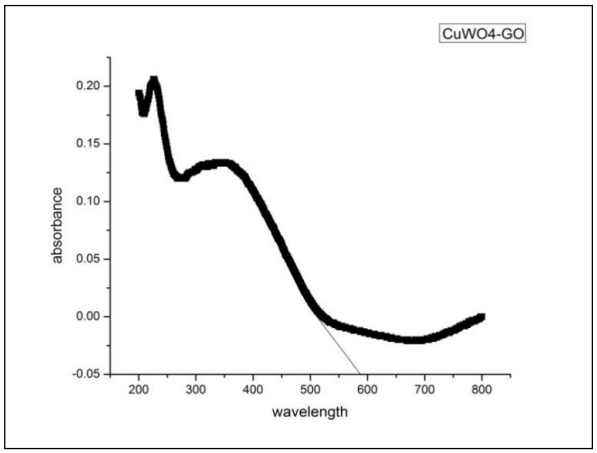

Figure 7: Band gap spectrum of Ag-$CuWO_4$ nano composite

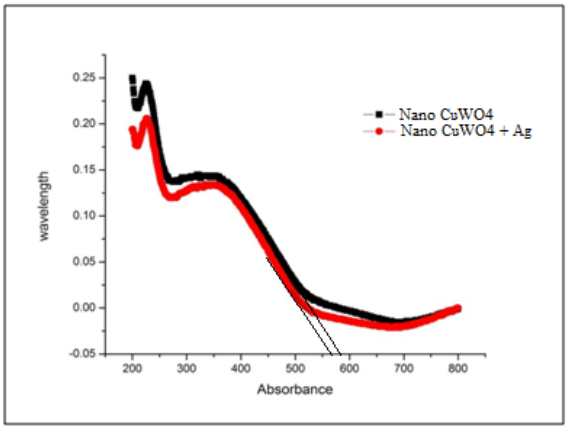

Figure 8: Band gap overlay spectrum of nano $CuWO_4$, Ag-$CuWO_4$ nano composite

International Journal of Multidisciplinary Advanced Research Trends (IJMART)
A Peer Reviewed (Referred) International Journal
http://ijmart.in/
Email: editor.ijmart@gmail.com
ISSN : 2349-7408
Vol. VII, Issue 2(1)
(AUGUST - 2020)

Table 1: Wavelengths and band gaps of $CuWO_4$, nano $CuWO_4$, Ag-$CuWO_4$ nano composite

Sample	Wavelength (nm)	Band Width (eV)
$CuWO_4$(metathesis)	295	4.20
Nano $CuWO_4$(Ball milled)	560	2.22
Ag-$CuWO_4$ nano composite	585	2.12

Raman Spectral Analysis

Raman spectrum of Ag-$CuWO_4$ nano composite is shown in **Figure 9**. Based on group theory, it can be concluded that wolframite structure with P_2/c (z =2) monoclinic structure gives 18 ($8A_g$ + 10 B_g) Raman-active bands out of 36 probable lattice modes. The Raman modes Ag-$CuWO_4$ exhibits the vibrations at 910 cm^{-1} which is a proof for wolframite type structure.

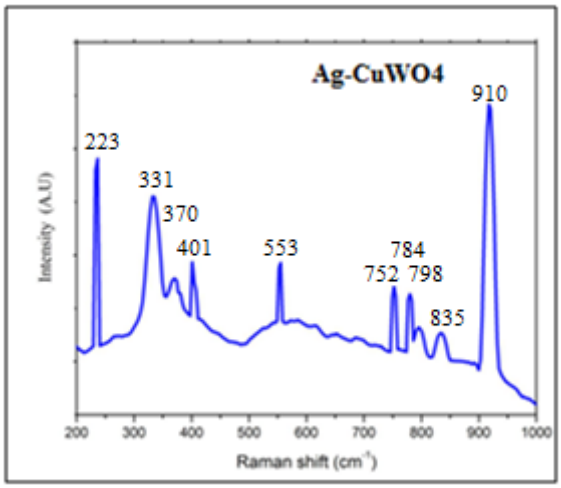

Figure 9: Raman spectra of Ag-$CuWO_4$ nano composite

UV-Visible Absorption spectra of Dyes:

The high intensity peaks were obtained at 667 nm and 617 nm respectively for Congo Red and Alizarin Red dyes, as shown by **Figure 10** and **Figure 11**. The percentage degradation of Congo Red and Alizarine Red was carefully monitored at different time intervals.

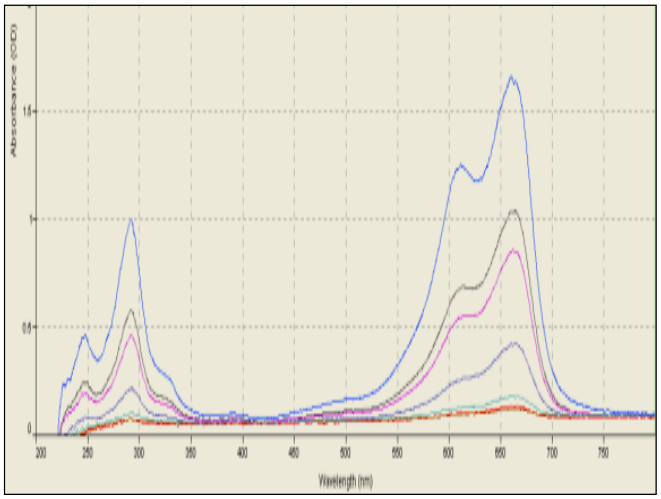

Figure 10: Absorption spectrum of Congo Red (λ_{max} at 667 nm)

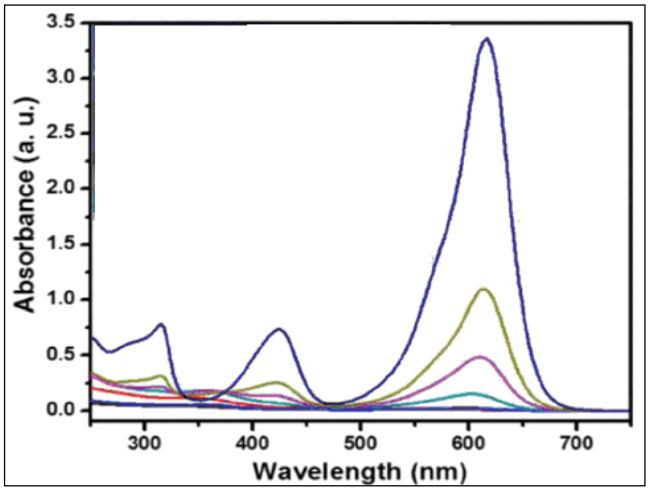

Figure 11: Absorption spectrum of Alizarine Red (λ_{max} 617 nm)

Photo Catalytic Activity Studies

The study of photo catalytic capability of the nano Ag-$CuWO_4$ composite was done by the degrading organic dyes Congo Red (CR) and Alizarine Red (AR)irradiated by visible light as depicted in **Figures 12, 13** and **14**, shown in comparison with micro and nano $CuWO_4$.

International Journal of Multidisciplinary Advanced Research Trends (IJMART)
A Peer Reviewed (Referred) International Journal
http://ijmart.in/
Email: editor.ijmart@gmail.com
ISSN : 2349-7408
Vol. VII, Issue 2(1) (AUGUST - 2020)

A sufficient time of around 30 minutes was allowed to establish the adsorption-desorption equilibrium between the photocatalyst and the dye. After a time span of 30 minutes, the reaction mixture is irradiated by visible light under continuous magnetic stirring, and the aliquot of the reaction mixture is taken every 10 minutes and subjected to UV-Visible analysis. As the reaction proceeded with Ag-$CuWO_4$ as the photocatalyst, the intensity of the absorption peaks was lowered. The final observation is that the AR dye solution is fully degraded in 60 minutes and CR dye solution in 80 minutes

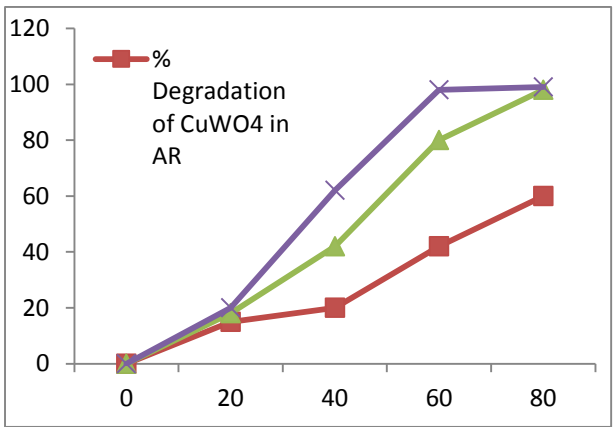

Figure 12: Photo degradation plots of Alizarine Red with copper tungstate, nano copper tungstate and silver-copper tungstate nano composite

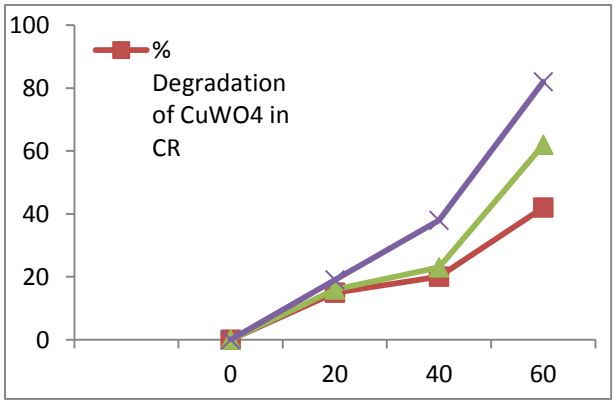

Figure 13: Photo degradation plots of Congo Red with copper tungstate, nano copper tungstate and silver-copper tungstate nano composite

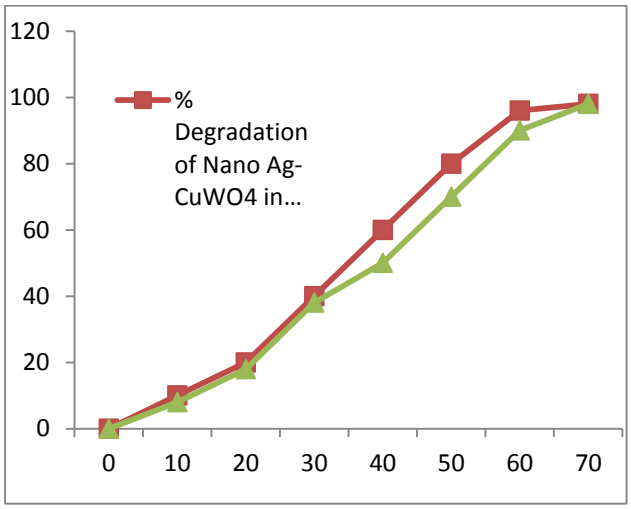

Figure 14: Photo degradation plots of Alizarine Red and Congo Red with nano silver-copper tungstate composite

Effect of % composition of Silver on the photocatalytic activity

Ag easily adsorbs Alizarine Red and Congo Red dye compared to $CuWO_4$. The adsorption capability of $CuWO_4$ has improved when Ag was incorporated on it. The degradation of AR & CR under visible light irradiation was studied using pure copper tungstate and modified copper tungstate by silver with various percentage compositions. In the absence of the catalyst, there is almost no photodegradation. Alizarine Red and Congo Red dyes had degraded in 80 to 100 minutes under irradiation of visible light in the presence of nano copper tungstate. The photocatalytic degradation of Alizarine Red and Congo Red dyes was enhanced by the Ag-$CuWO_4$ nano composite. By increasing the amount of silver nano particles from 1% to 5% in the Ag-$CuWO_4$ composite, the efficiencies of dye degradation were greatly raised from 80% to 100% in a time span of 60 to 80 minutes. The degradation efficiency remained the same even after adding 20% of silver in the composite, which is shown in **Figure 15**. It is concluded that the sample containing 5% silver in the Ag-$CuWO_4$ composite acts as the best in

International Journal of Multidisciplinary Advanced Research Trends (IJMART)
A Peer Reviewed (Referred) International Journal
http://ijmart.in/
Email: editor.ijmart@gmail.com
ISSN : 2349-7408
Vol. VII, Issue 2(1) (AUGUST - 2020)

eliminating the organic pollutants in wastewater using visible light irradiation.

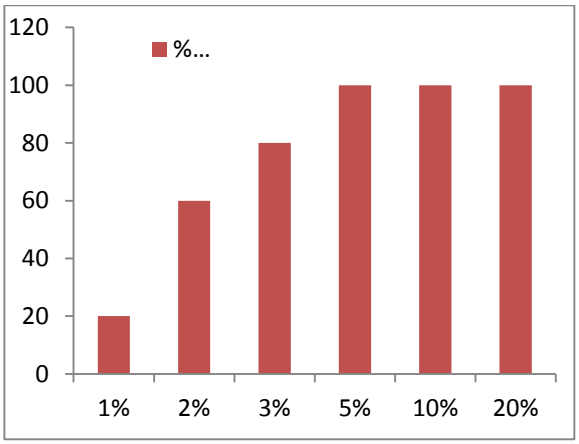

Figure 15: % of Ag Composition on catalyst

Effect of the amount of Ag-CuWO$_4$ nano composite

Figure 16 shows the influence of dosage of photocatalysts (10 mg of Ag-CuWO$_4$ nano composite) on the degradation of Alizarine Red (AR) and Congo Red (CR).At room temperature, observations were carried out by varying the dosage amount from 10 mg to 100 mg/100 lathe degradation efficiencies were greatly improved as the dosage of the catalyst was increased from 10 mg to 50 mg/100 ml. When the dosage of the catalyst increases, the reactive sites increase and as a result, more reactive oxidative species are produced. However, with excessive photocatalysts, the degradation efficiency of AR & CR reduces due to increase in light scattering and decrease in light penetration[27]. It illustrates similar percentage of degradation performed by 50 mg and 100 mg Nano Ag-CuWO$_4$ nano composite. Hence 50 mg Nano Ag-CuWO4 composite was only used in the experiment.

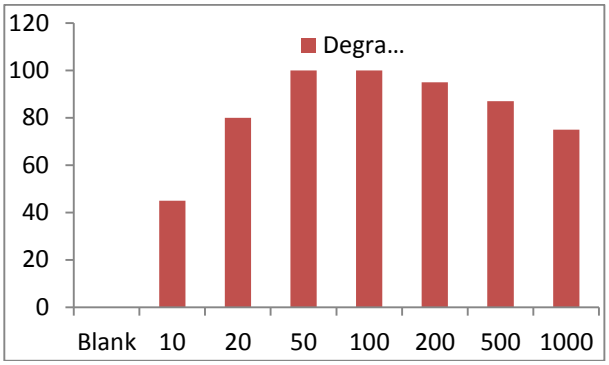

Figure 16: Effect of amount of Ag-CuWO$_4$ nano composite

Effect of Initial Dye Concentration

The influence of initial dye concentration on the degree of photodegradation was studied by varying the initial concentration over a range of 0.01 mg to 0.05 mg. The dye degradation rate is decreased with a rise in the concentration of the dye. This prompts us to enhance the dose of the catalyst or time span for the whole removal. The time vs. degradation percentage graphs of the dye (CR/AR) at different concentrations are shown in **Figure 17**. It can be explained that as the initial concentration of the dye raises, the solution becomes more intense coloured and the path length of incoming photons into the solution decreases. It infers that only fewer photons are reached on the surface of the catalyst [28].This influence was noticed by Matthews [29] during the photocatalytic degradation of Congo Red dye using Titania as catalyst. This indicates that the degradation requires more surface of the catalyst as the initial concentration of the dye increases. The OH radical which is the primary oxidising agent, produced on the surface of ZnO too is constant as the illumination time and the amount of catalyst are constant, Hence, as the quantity of catalyst increases, the number of free radicals striking the dye molecules decrease comparatively [30].As the concentration of dye increases, the rate of degradation decreases. This is due tithe retardation of penetration of light. It was found

International Journal of Multidisciplinary Advanced Research Trends (IJMART)
A Peer Reviewed (Referred) International Journal
http://ijmart.in/
Email: editor.ijmart@gmail.com
ISSN : 2349-7408
Vol. VII, Issue 2(1) (AUGUST - 2020)

that the percentage degradation rate decreased by increasing the concentration of dye solution from 5 to 100 ppm. Degradation was 90% at 5 ppm dye concentration, and it was reduced to 52% at 100 ppm dye concentration [31].

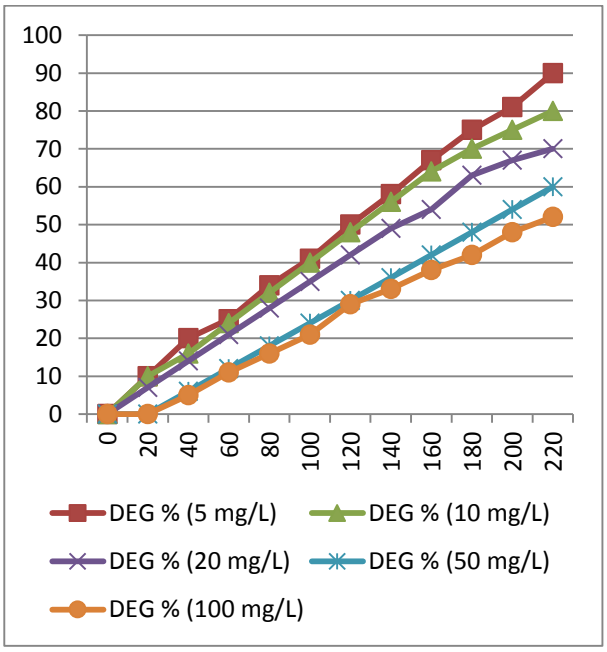

Figure 17: Effect of Initial Dye Concentration

Effect of pH of Initial dye Solution

The influence of pH on the photocatalytic degradation of the dye AR/CR in presence of Ag-$CuWO_4$ irradiated by visible light was studied. It was concluded that, the adsorption of dye AR/CR on the photocatalyst may be reduced as the pH of the dye AR/CR solution increases. This lead to enhancement of degradation and remained stable when pH of the AR solution raised from 5 to 7, and for CR solution raised from 3 to 5 when compared to the other pH values [32]. The transformation of $CuWO_4$ damages the Ag-$CuWO_4$ structure and in due coursedecreases the photocatalytic activity which is shown in **Figure 18**.

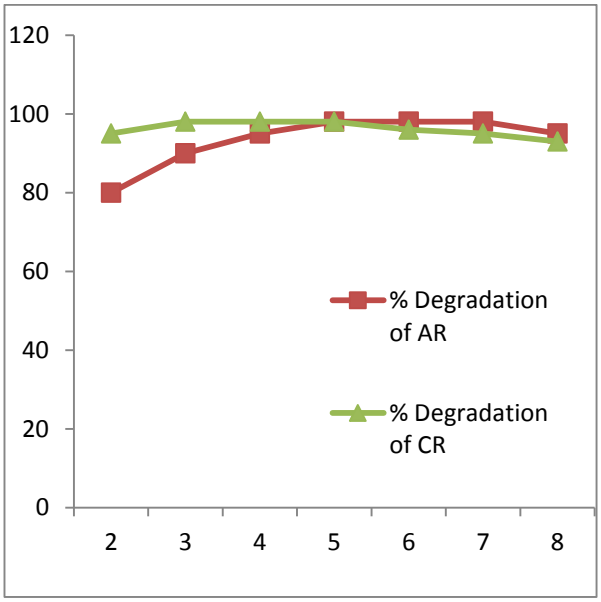

Figure 18: pH range of Ag-$CuWO_4$ Nano composite on Alizarine Red and Congo Red

Effect of Temperature

By varying the temperature from 0 to 80 °C, its impact on the photocatalytic capabilities of the samples irradiated by visible light was studied. The photocatalytic capabilities in the degradation of dye AR/CR were similar in the range of 20–60 °C and only slightly increased with increase in temperature. But the photocatalytic activity was greatly reduced when the temperature was maintained at 0 °C. This may be probably due to decrease in the mass of pollutants transferred to the surface of the photocatalysts and the lowering of production rate of oxidative species. The photocatalytic activity was significantly decreased at a temperature as high as 80 °C, which is shown in **Figure 19**. At high temperatures, charge carriers recombine and the adsorbed organics desorb from the photocatalysts. From these results, we can conclude that solar devices need temperature controller.

International Journal of Multidisciplinary Advanced Research Trends (IJMART)
A Peer Reviewed (Referred) International Journal
http://ijmart.in/
Email: editor.ijmart@gmail.com
ISSN : 2349-7408
Vol. VII, Issue 2(1)
(AUGUST - 2020)

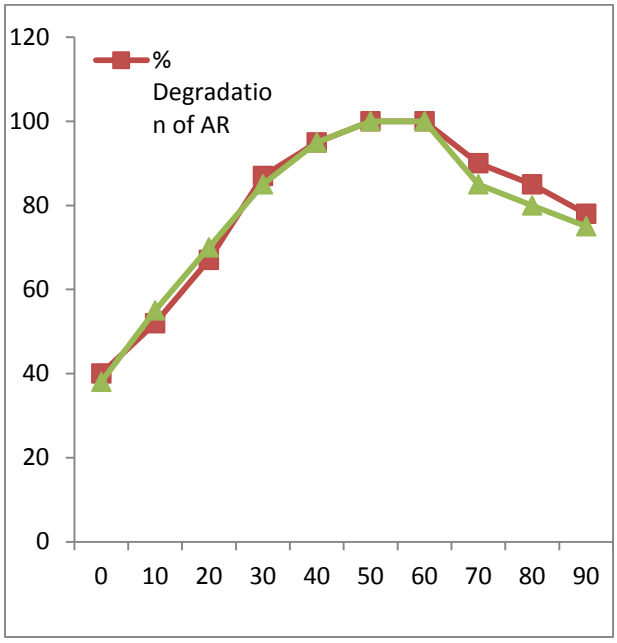

Figure 19: Temperature effect of Ag-$CuWO_4$ Nano composite with Alizarine Red and Congo Red

Reusability of the Catalyst:

By recycling Ag-$CuWO_4$ composite three times and the profiles of AR/CR concentrations, the reusability of the prepared sample was ascertained. In the first run, the efficiency of removal of the dye (AR) was 95%; in second run, it was 60% and in the third run, it was 30% over 80-160 minutes. In the first run, the efficiency of removal of the dye (CR) was 89%; in second run, it was 59% and in the third run, it was 22% over 80-160 minutes as shown, irradiated by visible light which is depicted in **Figure 20**. This little lowering of degradation efficiency happens because some amount of photocatalyst is lost between the two runs and also refractory intermediates get adsorbed on their surface [33]. In spite of this, the stability of the reused Ag-$CuWO_4$ photocatalysts after the degradation of dye (AR/CR) is still prominent.

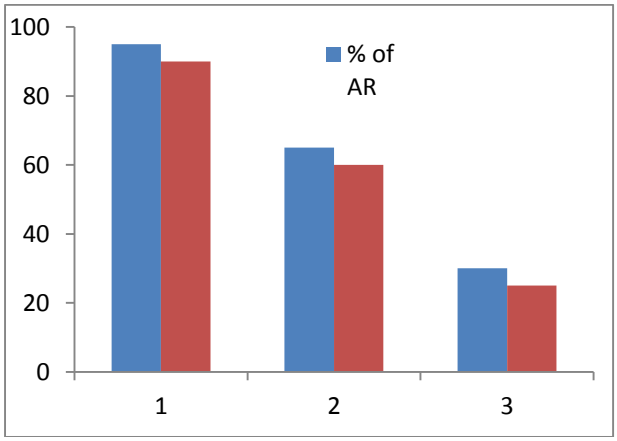

Figure 20: Reusability capacity of Ag-$CuWO_4$ Nano composite Alizarine Red and Congo Red

Plausible Photocatalytic Mechanism

The probable mechanism for the photocatalytic activity of the catalyst can be explained based on the presence of π-conjugation and 2D planar structures of silver in the Ag-$CuWO_4$ composite which can adsorb molecules of organic nature easily on its surface by means of powerfulπ-π interactions [34].In addition, the charge carrier mobility of silver is high and can be considered as an electron acceptor. It can cause significant lowering in the recombining rate of photo generated and holes. On being excited by visible light, the electron-hole pairs are produced on the copper tungstate-silver surface. Subsequently, the immediate transfer of photo generated electrons onto silver takes place by means of a percolation mechanism. Then silver possessing negatively charge is able to activate the dissolved oxygen producing superoxide radical, whereas the holes could react with the water adsorbed, forming hydroxyl radical. Ultimately, the Congo Red and Alizarine Red dye molecules which got adsorbed on the active sites of the copper tungstate-silver system through the π-π stacking and electrostatic attraction are oxidised by the active species, holes, superoxide anion radical and hydroxyl radical, as shown in **Scheme 1**.

International Journal of Multidisciplinary Advanced Research Trends (IJMART)
A Peer Reviewed (Referred) International Journal
http://ijmart.in/
Email: editor.ijmart@gmail.com
ISSN : 2349-7408
Vol. VII, Issue 2(1) (AUGUST - 2020)

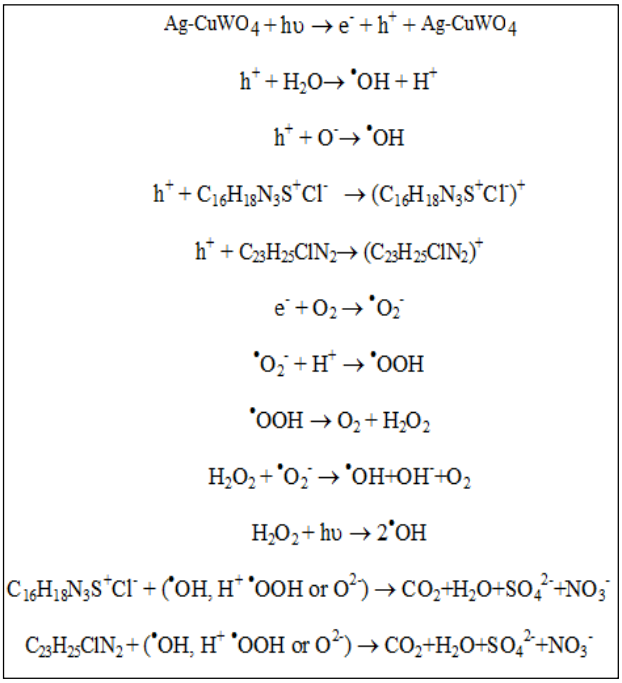

Scheme 1: Photochemical Mechanism of the catalysts with the dyes

Conclusion

Here we report the successful synthesis of silver-copper tungstate nano composite by colloidal blending process. Ag-$CuWO_4$ nano composite has been presented to exhibit excellent photocatalytic degradation with Congo Red and Alizarine Red dyes under visible light irradiation. The XRD, FESEM, EDS illustrates the morphology and structure of the prepared sample in detail. The complete degradation of Congo Red dye took place in 60 minutes and Alizarine Red in 80 minutes irradiated by visible light, using nano composite Ag-$CuWO_4$ as the photo catalyst. This result suggests that as-obtained nano crystalline Ag-$CuWO_4$ composite is found as favourable material having high potential to be used for photo catalytic applications under visible light.

References

1. Honda K; Fujishima A, *Nature*, **1972**, 238, 37.
2. Hoffmann MR; Martin ST; Choi W; Bahnemann DW, *Chem. Rev.*,**1995**,95**,** 69.
3. Li FB; Li XZ; Hou MF, *Appl. Catal.*, ***B,*** **2004,** 48, 185.
4. Chamberland BL; Kafalas JA; Goodenough JB, *Inorg. Chem.*, **1977**, 16, 44.
5. Gillette RH, *Rev. Sci. Instrum.*, **2014**, 21, 508.
6. Gopalakrishnan J; Sivakumar T; Ramesha K; Thangadurai V; Subbanna GN, *J. Am. Chem. Soc.*, **2000**, 122**,** 6237.
7. SivakumarT; Lofland SE; Ramanujachary KV; Ramesh K; Subbanna GN; Gopalakrishnan J, *J. Solid State Chem.*, **2004**, 177**,** 2635.
8. Mandal TK; Gopalakrishnan J, *J. Mater. Chem.*, **2004**, 14**,** 1273.
9. Mani R; Bhuvanesh NSP; Ramanujachary KV; Green W; Lofland SE; Gopalakrishnan J, *J. Mater. Chem.*, **2007**, 17, 1589.
10. Gillan EG; Kaner RB, *J. Mater. Chem*, **2001**, 11, 1951.
11. Wiley JB; Gillan EG; Kaner RB, *Mater. Res. Bull.*, **1993**, 28**,** 893
12. Ruiz-Fuertes J, *Phys. Rev. B.* **2010**, 81**,** 224115.
13. Yourey JE; Bartlett BM, *J. Mater. Chem.*, **2011**, 21, 7651.
14. Chang Y; Braun A; Deangelis A; Kaneshiro J; Gaillard N, *J. Phys. Chem. C,* **2011**, 115, 25490.
15. Jeong SH; Yeo SY; Yi SC; *J. Mater. Sci.*, **2005,** 40, 5407 - 5411.
16. Choi O; Deng KK; Kim NJ; Ross L.Jr; Surampalli RY; Hu Z, *Water Res.*,**2008,** 42, 3066 - 3074.
17. Rai M; Yadav A; Gade A, *Biotechnol. Adv.*, **2009** 27, 76 - 83.

18. Jain PK; Huang X; El-Sayed IH; El-Sayed MA, *Acc. Chem. Res.*, **2008,** 41, 1578 - 1586.
19. Nair LS; Laurencin CT, *J. Biomed. Nanotech.*, **2007,** 3,301-316.
20. Natarajan K; Selvaraj S; Ramachandra MV, *Dig. J. Nanomater. Biostructures,* **2010,** 5, 135 - 140.
21. Gopinath V; MubarakAli D; Priyadarshini S; Priyadharshini NM; Thajuddin N; VelusamyP, *Colloids Surf. B.*, **2012,** 96, 69 - 74.
22. Mohanpuria P; Rana NK; Yadav SK, *J. Nanoparticle Res.*, **2008,** 10, 507 - 517.
23. Wan-Kuen Jo; Hyun-Jung Kang, *Powder Technol.*, **2013**, 250, 115.
24. Chao Wei; Ying Huang; Xin Zhang; Xuefang Chen; Jing Yan, *Electrochim. Acta*, **2013**, 220**,** 156.
25. Muthamizh S; Suresh R; Giribabu K; Manigandan R; Praveen S, *AIP Conf. Proc.*, **2014**, 1591, 508.
26. Hu X; Meng X; Zhang Z,*Int. J. Photoenergy*, **2016,** 1155, 10.
27. Meng X; Zhan Z, *Int. J. Photoenergy*, **2015**, 1155, 10.
28. Davis RJ; Gainer JL; Neal GO; Wenwu I, *Water Environ. Res.*, **1994**, 66**,** 50.
29. Matthews RW, *J. Chem. Soc., Faraday Trans*, **1989**, 85, 1291.
30. Mengyue Z; Shifu C; Yaown T, *J. Chem. Tech. Biotechnol.*, **1995**, 64, 339.
31. PinkySK; Ferdush A; Kurny ASW; Gulshan F, *IJIRSET* **2015**, 4,9986.
32. Meng X; Jiang L; Wang W; Zhang Z, *IJIRSET* **2015,** 9, 747024.
33. Huang H; Zhen S; Li ; Tzeng S; Chiang H, *Opt. Express,* **2016**, 24, 14.